Available online at www.sciencedirect.com

SCIENCE DIRECT®

Earth and Planetary Science Letters 229 (2004) 61–71

EPSL

www.elsevier.com/locate/epsl

Evidence of a slab of subducted lithosphere beneath central Taiwan from seismic waveforms and travel times

Po-Fei Chen*, Bor-Shouh Huang, Wen-Tzong Liang

Institute of Earth Sciences, Academia Sinica, Nankang, Taiwan

Received 7 November 2003; received in revised form 18 October 2004; accepted 19 October 2004
Available online 19 November 2004
Editor: R.D. van der Hilst

Abstract

Knowing whether there is a slab of subducted lithosphere beneath central Taiwan is important for our understanding of the regional tectonic evolution. In this study, we aim at resolving this issue by investigating the seismic effects of a potential near-receiver slab, using data from a local broadband array. Rays from deep and intermediate-depth earthquakes in the Tonga–Kermadec subduction zone to central Taiwan stations exhibit reduced amplitudes and travel times relative to KMNB in the 0.1–0.4 Hz band, with a correlation between the degree of reduction and earthquake latitudes. The overall amplitude reduction observed at central Taiwan stations is not observed for earthquakes from the Hindu Kush. Our analysis suggests that the observations are not caused by crustal structure but by receiver-side heterogeneous mantle or, more specifically, an eastern dipping aseismic slab beneath central Taiwan. The extent of the slab is determined by jointly modeling amplitude and travel time observations at SSLB and TPUB using a 2-D pseudospectral method.

Keywords: Tonga–Kermadec; subduction zone; seismic wave

1. Introduction

Whether or not a slab of subducted lithosphere exits between 23°N and 24°N beneath central Taiwan remains an open question. Subduction zone seismicity does not provide conclusive answers because no earthquakes occur beyond ~80-km depth. Models published thus far adopt different views on the issue. For instance, in terms of tectonic evolution, the model of arc–continent collision [1–4] supports the presence of a slab, whereas that of arc–arc collision [5] favors its absence. In terms of orogenic processes, the model of skinned collision [6] or crustal exhumation [7] assumes its presence, whereas that of lithospheric collision [8] advocates its absence. Therefore, the resolution of the debate is crucial to a better understanding of the tectonic evolution and orogeny in the

* Corresponding author. Now at Seismological Center, Central Weather Bureau, Taiwan.
E-mail address: bob@scman.cwb.gov.tw (P.-F. Chen).

0012-821X/$ - see front matter © 2004 Elsevier B.V. All rights reserved.
doi:10.1016/j.epsl.2004.10.031

region. Although its presence has been suggested by results of global tomography [4], the evidence is relatively indirect because of deterioration of resolution at depth [4] and because of the integrated nature of travel time anomalies in global studies.

Seismic wave propagation is faster in a subducting slab than in ambient mantle. A seismically fast slab acts as an antiwaveguide, diffracting away high-frequency energy [9]. As a result, seismic waves propagating through a slab exhibit earlier arrivals, smaller amplitudes, and broader waveforms [9]. Travel time residuals [10] and waveform anomalies [11,12] are primary tools to investigate globally the ultimate depth of subducting slabs; here, we apply them to probe the existence or absence of a slab beneath central Taiwan. In this study, we aim at providing more direct evidence by investigating the first P amplitudes and arrival times of deep and intermediate-depth earthquakes from the Tonga–Kermadec subduction zone as recorded by the "Broadband Array in Taiwan for Seismology" (BATS), using the station offshore of mainland China, KMNB, as a reference station.

The seismic effects of a near-receiver slab can be observed with a seismic array above the subducting slab. As Fig. 1 illustrates that for a common teleseismic source, the near-source paths are nearly the same, so that discrepancies of two observations at the BATS array mainly stem from receiver-side heterogeneities in mantle structure and their corresponding crustal effects. In contrast to studies examining waveform effects of a near-source slab [11,12], corrections for the differential path effects, geometrical spreading, attenuation, and source radiation patterns are unnecessary. Furthermore, this approach is relatively insensitive to errors in source location. To isolate the slab signatures, the only correction required concerns crustal effects at different stations.

First, the frequency range of seismic signals is determined from two example earthquakes. Second, within the frequency band thus determined, whether or not the seismic waveforms and travel times of all other earthquakes exhibit consistent patterns is examined. We remark that for the frequency of interest, the Fresnel zone corresponds to the thickness of the hypothetical slab. The derived waveform and travel time patterns, if any, are then compared with those predicted from slab effects. Finally, using a 2-D pseudospectral method [13], we model the joint patterns of seismic amplitudes and travel times with a 100-km-thick planar slab. Results of this study indicate that the observations are consistent with the presence of a slab, which, upon modeling, ranges from 400-km-long, 4% velocity anomaly to 500-km-long, 3.2% velocity anomaly.

2. Data analysis

The deployment of BATS in the mid 1990s [14] and the peculiar geometrical relationship between

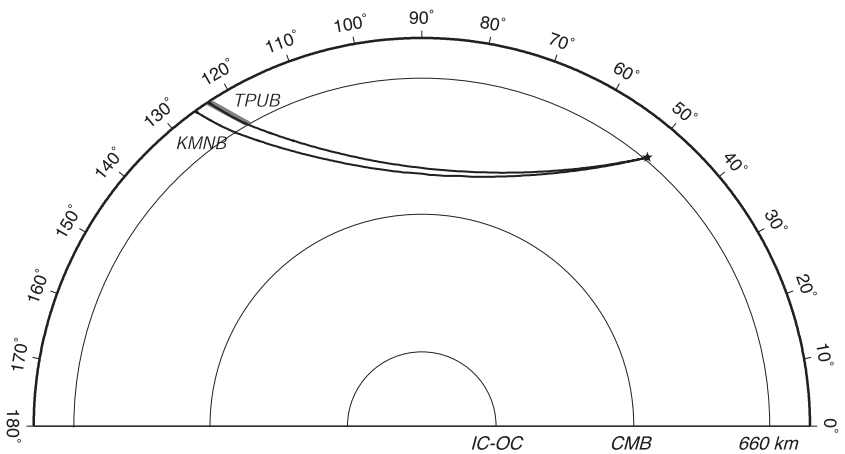

Fig. 1. Ray paths of first P from a Tonga–Kermadec event to TPUB and KMNB. Note that a P wave arriving at TPUB would travel through the possible 60° dip, 100-km-thick slab (stippled), but miss the slab entirely at KMNB.

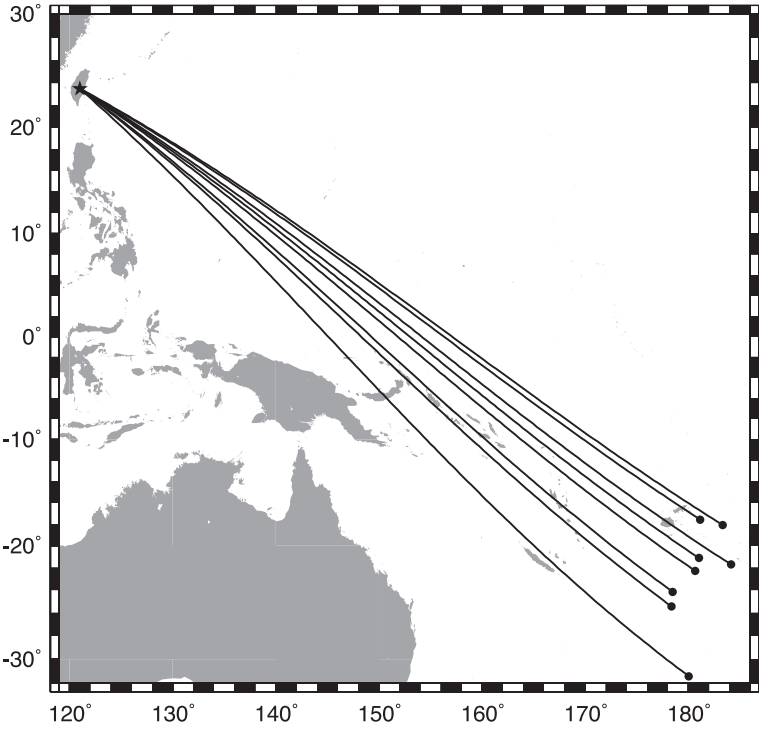

Fig. 2. Great circle paths of the eight Tonga–Kermadec earthquakes to TPUB. Note the earthquakes used span more than 10° in epicentral latitude, ensuring latitude variation of P amplitudes at any specific station in BATS.

Taiwan and Tonga–Kermadec make our application feasible. Fig. 1 is a great circle section showing two ray paths from a common deep source in the Tonga–Kermadec subduction zone to the two BATS stations (TPUB and KMNB; refer to Fig. 6 for their locations). TPUB is on the main Taiwan island, while KMNB is off coast of SE China (Kinmen island). The dip angle of the slab in Fig. 1 is assumed to be 60°, as extrapolated from that of the Luzon arc [15]. We further assume the slab thickness as 100 km, that it extends to 600-km depth, and that the station TPUB projects to the center of the slab.

The reasons for choosing earthquakes from the Tonga–Kermadec subduction zone are threefold: (1) suitable azimuth: the azimuths of Tonga–Kermadec events to Taiwan are between N120°E and N130°E (Fig. 2), comparable to the azimuth of the Eurasia–Philippine relative plate motion, and are nearly normal to the structural trend of the island (N20°E for the central range and the coastal range). If the strike of the potential slab parallels that trend, those azimuths are in a sense perpendicular to the strike, which legitimates the 2-D approximation (Fig. 1). This 2-D scenario also minimizes the differential slab effects due to minor azimuthal variations of earthquakes. (2) Suitable epicentral distance: as Fig. 1

Table 1
Earthquakes used in this study (Harvard CMT catalogue)

No.	Centroid parameters									
	Date			Time			Latitutde	Longitude	Depth	M_o (10^{25})
	Y	M	D	h	m	s	λ	ϕ	h	dyne cm
1[a]	1998	3	29	19	48	16.2	−17.57	−178.85	554.0	64
2	1998	5	16	2	22	3.2	−22.27	−179.35	609.0	23
3	1998	12	27	0	38	26.8	−21.69	−175.86	160.0	20
4	2000	6	14	2	15	25.8	−25.45	178.38	615.0	5
5[a]	2000	8	15	4	30	8.8	−31.42	−179.95	367.0	9
6[b]	2000	12	18	1	19	21.6	−21.11	−178.98	656.0	7
7	2001	4	28	4	49	53.4	−18.07	−176.68	367.0	21
8	2002	8	19	11	8	24.3	−24.16	178.49	699.0	430

[a] Example earthquakes for detailed frequency analyses.
[b] Discarded event.

shows, the epicentral distance between Taiwan and Tonga–Kermadec is about 75°. At such epicentral distances, incident rays would optimally sample a subducting slab with 60° dip angle, ensuring substantial slab effects to be detected. (Although the assumed 60° dip angle is extrapolated from that of the Luzon arc without rigorous proof, the ends will justify the means by our observations.) On the other hand, the long epicentral distance warrants that the ray paths to KMNB and the Taiwan island stations are similar on the source side with nearly the same take off azimuth, minimizing differential source effects. Furthermore, the bottom depths of rays for such epicentral distance are within lower mantle, eliminating the problem of multipathed P waves. (3) High seismic activity: the Tonga–Kermadec subduction zone is one of the most seismically active slabs in the world. The abundant deep and intermediate-depth earthquakes as recorded by BATS facilitate the compilation of any potential pattern(s) from observations.

Deep and intermediate-depth earthquakes of the Tonga–Kermadec subduction zone with simple and

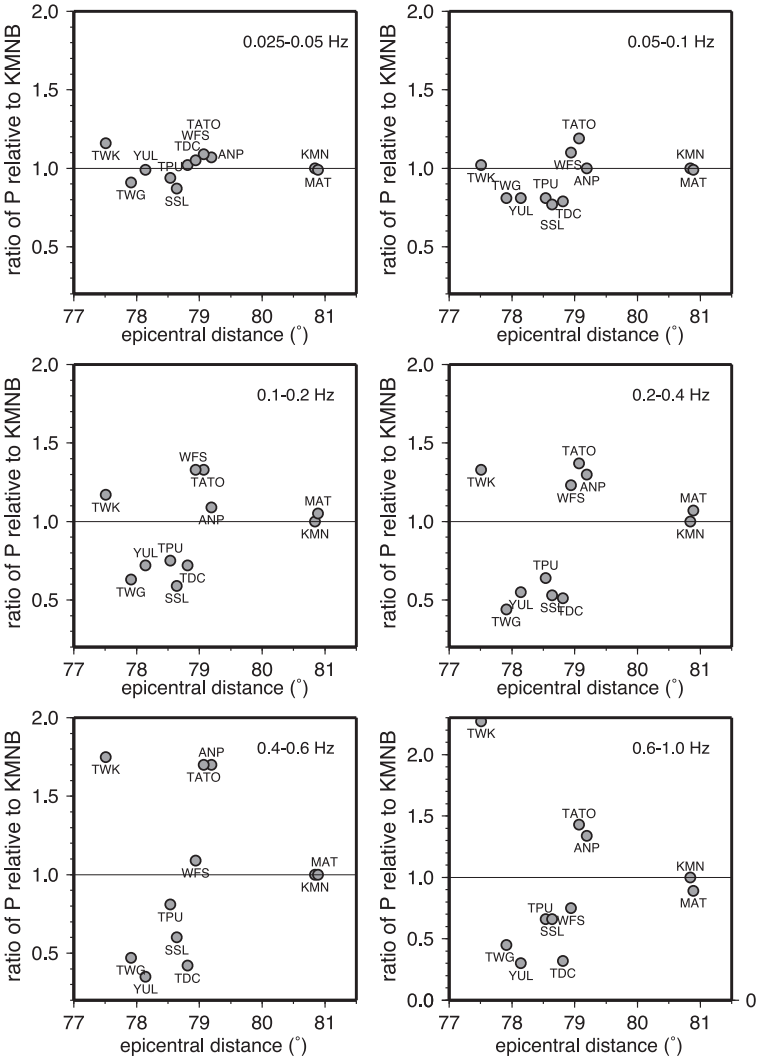

Fig. 3. Frequency-dependent variations of P amplitude ratios of BATS stations for the 20000815 event. The P ratios are comparable and close to one for low frequency energies (<0.1 Hz) but display significant deviations between 0.1 and 0.4 Hz.

sharp waveforms of first P arrivals are selected. A total of eight earthquakes were used in the analysis (Table 1), with their great circle paths shown in Fig. 2. The vertical components of velocity records are integrated and the instrumental response removed to obtain true ground displacements. For each event, the peak-to-trough magnitudes of first P is measured and represented by ratios relative to reference values at KMNB. The bandpass frequency range selected for the study is determined as follows. We conduct a detailed frequency-dependent analysis from two example earthquakes ("a" in Table 1). Results of

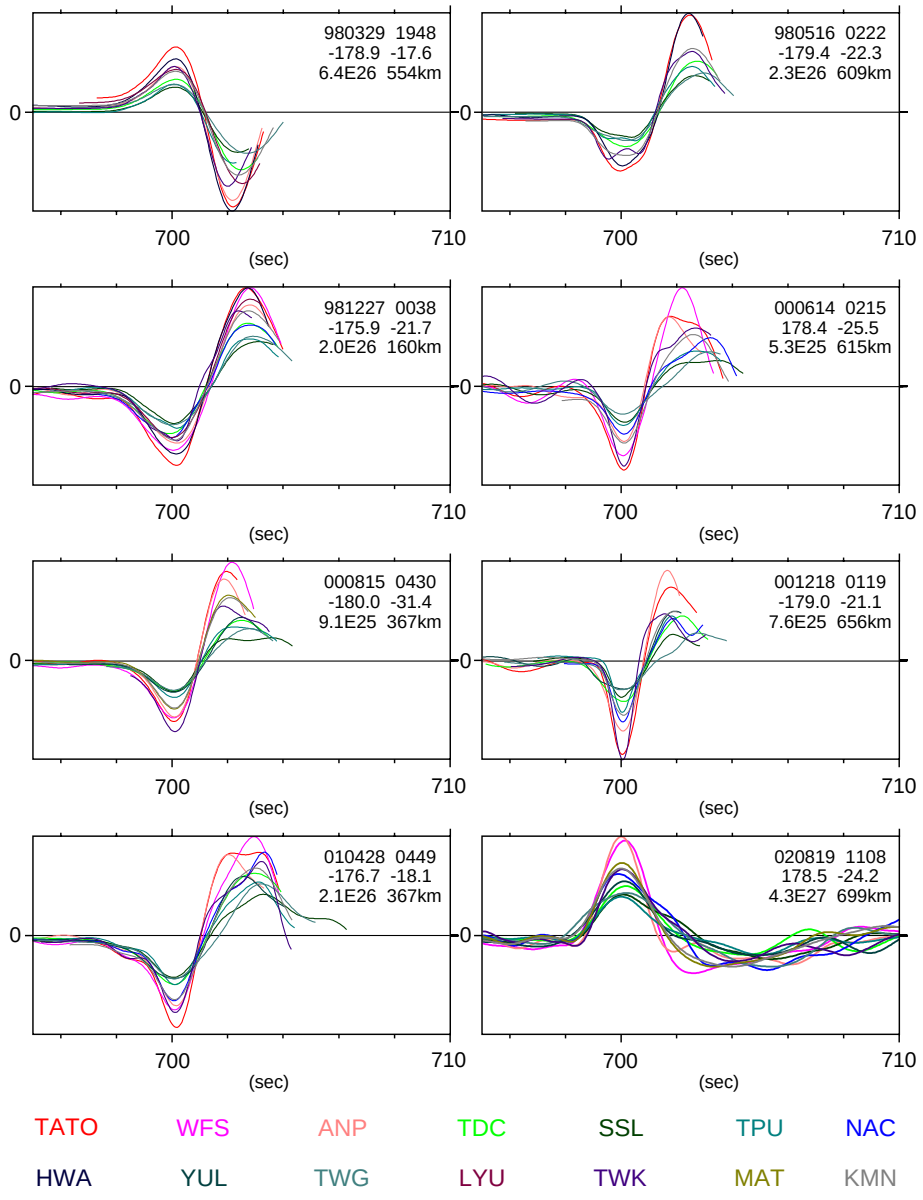

Fig. 4. P waveforms aligned at 700 s for each of the eight earthquakes with stations color-keyed. Note the similar color pattern for all eight earthquakes. Also note the waveforms are broader for those with smaller amplitudes. The earthquake parameters are shown in the box (refer to Table 1).

the analysis indicate comparable P ratios for low-frequency energy (<0.1 Hz) and significant deviations for signals between 0.1 and 0.4 Hz (Fig. 3). Comparable low-frequency energies suggest that the differential source effects are minimal at all stations, and the differences in geometrical spreading and anelasticity are negligible. The 0.1–0.4 Hz frequency range is adopted to bandpass the records of the eight earthquakes (Fig. 4).

As for travel time observations, we define the differential residual times (DRTS) relative to KMNB as:

$$\mathrm{DRTS}_{\mathrm{bats}} = \left(T^{\mathrm{obs}}_{\mathrm{bats}} - T^{\mathrm{the}}_{\mathrm{bats}}\right) - \left(T^{\mathrm{obs}}_{\mathrm{kmnb}} - T^{\mathrm{the}}_{\mathrm{kmnb}}\right) \qquad (1)$$

"*bats*" could be any BATS station; "*obs*" stands for observed travel time corrected for station elevations, whereas "*the*" represents theoretically calculated travel time from iasp91 [16].

3. Results

One event is discarded ("b" in Table 1) as its result is relatively inconsistent with others. For the remaining seven earthquakes, we show in Fig. 5 P amplitude ratios with solid circles and DRTS with triangles for each BATS station aligned from north to south. Due to a timing problem at KMNB for a short time span, some stations have more circles than triangles. Fig. 5 demonstrates that both amplitudes and travel times observed at any BATS station tend to display consistent anomalies relative to KMNB for nearly all deep and intermediate-depth earthquakes from the Tonga–Kermadec subduction zone. For comparison, the amplitude ratios relative to KMNB for earthquakes from the Hindu Kush are shown as open squares and will be discussed later. For the Tonga–Kermadec events, the consistent pattern exhibited by any specific station implies that the differences between stations with high P ratios (e.g., TATO) and low P ratios (e.g., TPUB) are real.

The averages and standard deviations of amplitude and travel time anomalies are calculated for each BATS station. Plotting the results at the locations of the corresponding stations reveals that the P amplitudes relative to those of KMNB are

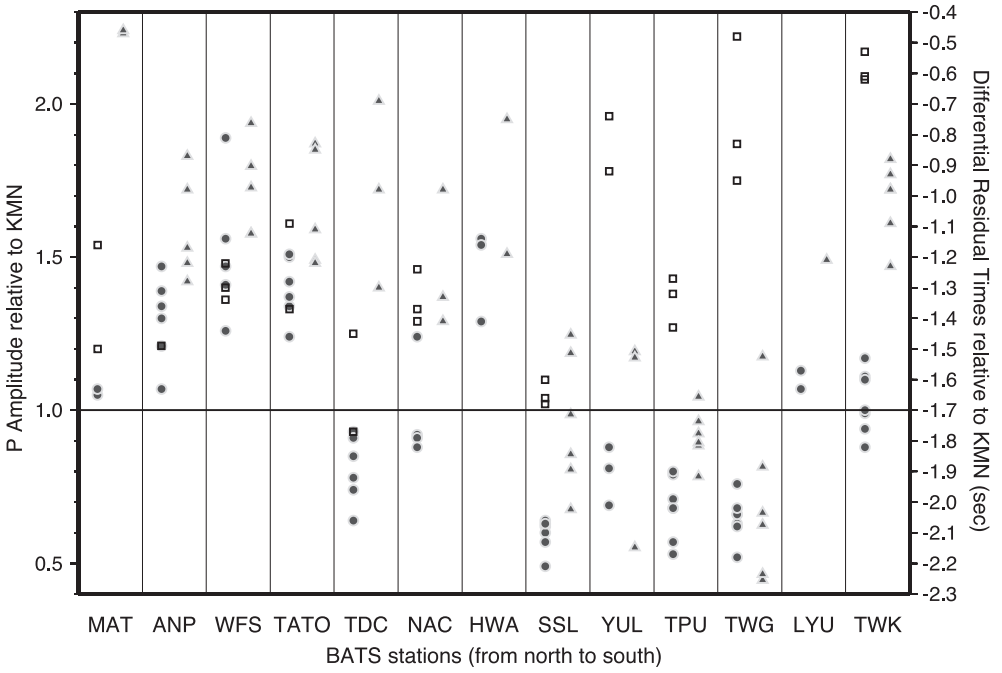

Fig. 5. P amplitude ratio (left scale) and differential residual times (right scale) relative to KMNB. Solid circles (●) are for P ratios, and solid triangles (▲) are for DRTS of the Tonga-Kermadec events. Open squares (□) are for P ratios of the Hindu Kush events. Note that the pattern of reduced amplitudes for central Taiwan stations from the Tonga–Kermadec events is absent from the Hindu Kush events.

unanimously high and low for stations in northern and central Taiwan, respectively (Fig. 6). Stations with reduced amplitudes have also the most negative DRTS. While the enhanced amplitudes of northern Taiwan stations (ANPB, WFSB, and TATO) and the short scale variation near Hualien (NACB and HWAB) might originate from the northward subduction of the Philippine Sea plate, we focus on observations of the central Taiwan stations (TDCB, SSLB, YULB, TPUB, and TWGB). The reduced amplitudes suggest that seismic rays from Tonga–Kermadec to central Taiwan sample either a receiver-side high-velocity anomaly in the mantle or a high seismic attenuation in the crust (or both). The following arguments will lead to the conclusion that the cause(s) is likely to originate from the mantle, and the high-velocity anomaly is likely to be an aseismic slab beneath central Taiwan.

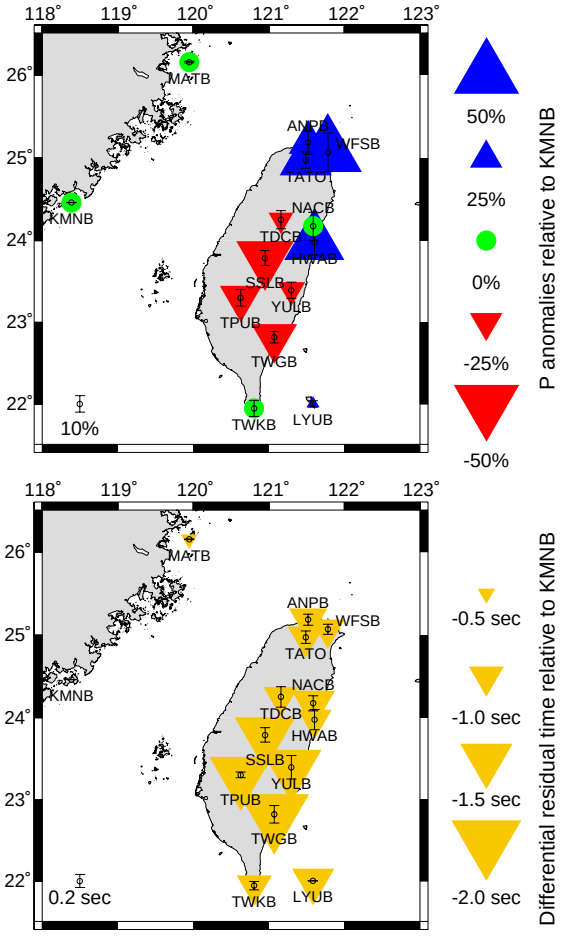

Fig. 6. Averages and standard deviations of amplitude and travel time anomalies of BATS stations relative to KMNB, plotted at station locations, for the Tonga–Kermadec events. Note the low P ratios and relatively negative DRTS for central Taiwan stations.

The clustering of central Taiwan stations around the mountain range raises the likelihood of attributing the observed patterns to crustal effects. Although the crustal effects can be corrected by observations of teleseismic events from other regions, both the complex mantle structure in the vicinity of Taiwan and the short time span of BATS have made a decisive correction currently unavailable. Instead of making a quantitative correction, we estimate whether the observations are dominated by anomalous crust or anomalous mantle. There are four arguments: (1) if the observed reduced amplitudes are a result of low Q crustal materials, those high-attenuation materials tend to be slow for seismic wave propagations. We would then observe positive DRTS. (2) If it is the crustal effects that dominate the anomalies, the observed patterns would be relatively independent of earthquake azimuths. However, the reduced amplitudes of central Taiwan stations as observed for the Tonga–Kermadec events are not reproduced for the Hindu Kush events from the west (Fig. 5). (3) The earthquakes used in this study span more than 10° in latitudes (Fig. 2), more than enough to sample a distinct mantle portion on the receiver side, while for any specific station, the crustal material sampled remains the same. We thus investigate potential relationships between P amplitude ratios and earthquake latitudes and find a linear positive correlation for central and southern Taiwan stations, which is not seen for stations in northern Taiwan (Fig. 7). For crustal effects to produce the correlation, the lateral heterogeneities would need to be unreasonably large. (4) The positive correlation between amplitudes and earthquake latitudes implies that, for any specific station in central or southern Taiwan, the mantle is colder to the south. This is consistent with the idea that the arc–continent collision is propagating southward because the ceased subduction to the north has warmed up the slab. In summary, the first three argue for the reduced amplitudes and travel times originating from a mantle anomaly, whereas the last suggests that the anomaly can be explained by an eastern dipping slab beneath central Taiwan. The slab effects

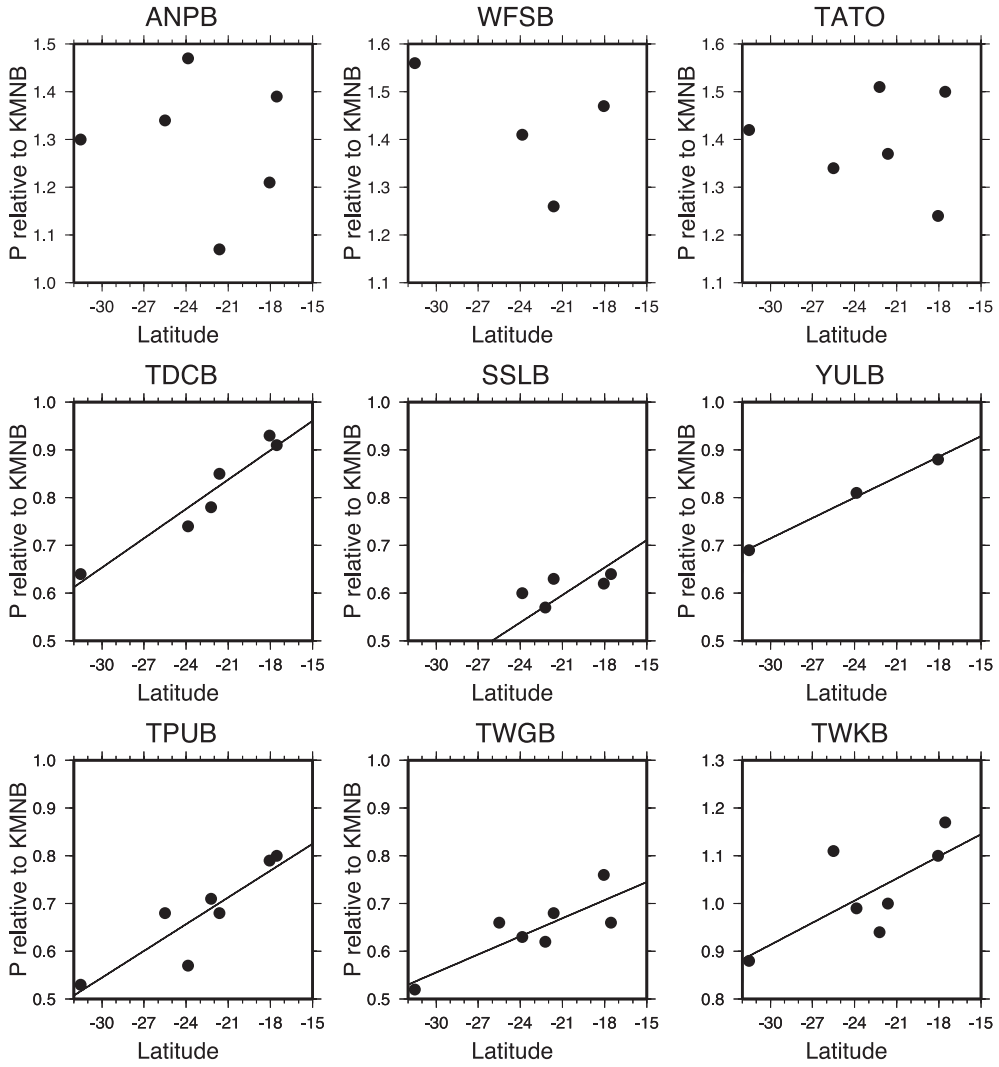

Fig. 7. P amplitude ratios relative to KMNB versus latitudes of the Tonga–Kermadec events for each of BATS stations. Note the positive correlation for central and southern Taiwan stations, which is missed for northern Taiwan stations.

can be observed as far north as 24.3°N based on the correlation of TDCB (Fig. 7), although its travel time anomaly is not as prominent as those of other central Taiwan stations.

4. Model observations by seismic effects of a planar slab

We use a 2-D pseudospectral method [13] to model the reduced amplitudes and travel times observed by simulating the seismic effects of a 100-km-thick planar slab. A plane wave with dominant frequency of 0.1 Hz propagates upwards with an incident angle complementary to the slab dip (Fig. 8). We set up a line of receivers near the surface. Based on the recorded waveforms of first arrival, we calculate ratios of maximum amplitude and differential travel times of the receiver at the center of the slab, relative to a reference station, for various combinations of slab length and velocity anomalies. We use iasp91 for

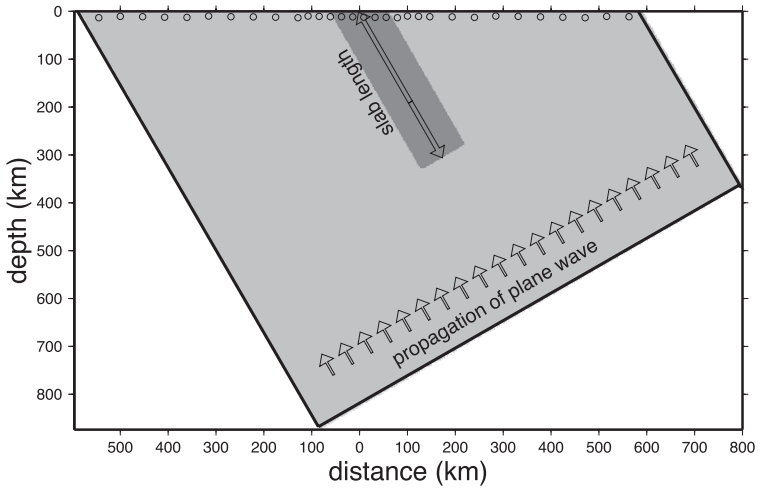

Fig. 8. 2-D simulation of plane wave propagations through a planar slab structure (dark zone). Circles represent receiver array near the surface.

the average velocity of the upper mantle [16]. The resultant amplitude ratios and travel time anomalies are then contoured with red dashed and blue dotted lines, respectively, in the plane of the two variables (Fig. 9).

We assume that SSLB and TPUB project at the center of the slab and superimpose their observed ranges of amplitudes and travel times on the contour figure, shown as bold, red dashed and bold, blue dotted lines, respectively (Fig. 9). The intersected area, colored in green, is then the probable range of slab properties jointly constrained by seismic amplitudes and travel times. We further extract the slab range of properties mutually shared by the observations of SSLB and TPUB, and denoted it with stars in Fig. 9. We conclude that amplitude and travel time anomalies observed at SSLB and TPUB require a slab ranging from 400-km-long, 4% velocity anomalies to 500-km-long, 3.2% velocity anomalies.

5. Discussion

Although we managed to estimate an overall range of the slab extent from observations, the realistic slab configuration is by no means resolved uniquely by our study because of the many assumptions that needed to be made: e.g., a rectangular slab shape, a purely elastic medium, no lateral variations in slab structure, and no crustal effects. Similarly, the locations of TPUB and SSLB are assumed to be at the center of the slab, and only the compatible parts of observations are used to constrain the slab. While the realistic configuration of the subducting slab needs more observations to be fully constrained, its existence beneath central Taiwan has been confirmed in this study as argued in the results.

Then, why are there no intermediate-depth earthquakes beneath central Taiwan? Lallemand et al. [4] have speculated that the possible reasons might be (1) hot, (2) ductile, and (3) mechanically detached from the upper part of the subducting slab. We would like to propose one more potential explanation. According to current models explaining the mechanism of intermediate-depth earthquakes [17–19], the effective normal stress is reduced by fluids liberated from dehydration reactions of subducted hydrous minerals, which favors a brittle behavior of the material in response to stresses in the slabs. In central Taiwan, the continents have been colliding with the arc, and the oceanic lithosphere has been consumed entirely by subduction. Under the circumstances, no available hydrous minerals will be freshly supplied for dehydration reactions through subduction processes, resulting in no intermediate-depth earthquakes. As

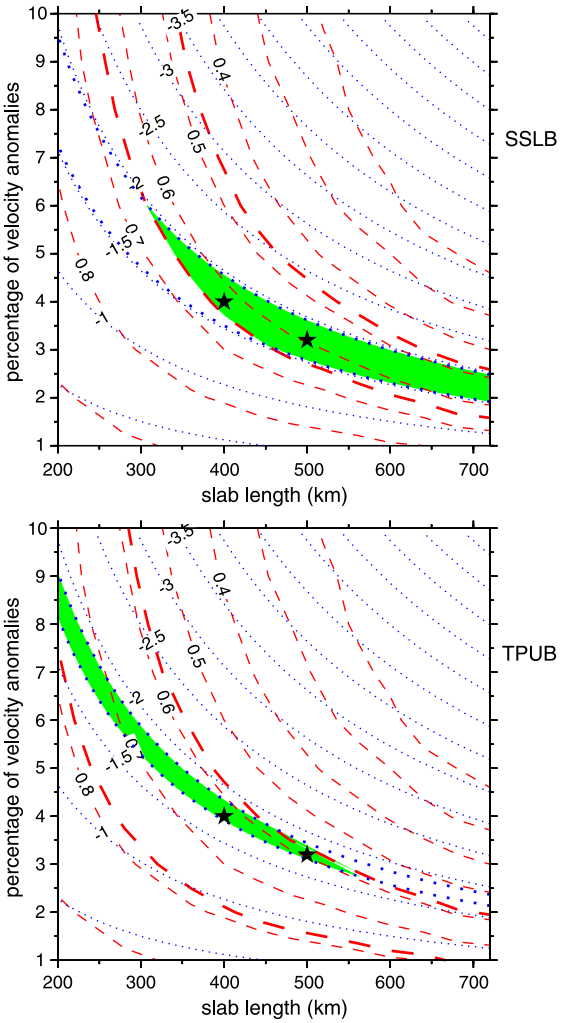

Fig. 9. Contoured amplitude ratios (red dashed lines) and travel time anomalies (blue dotted lines) as a function of velocity anomalies and slab length for receiver at the center of the slab relative to those undisturbed. Bold symbols indicate the range of corresponding observations at SSLB (Top) and TPUB (bottom), respectively. The ranges mutually shared by amplitude and travel time observations are colored in green. Stars further indicate the range mutually compatible with the observations at SSLB and TPUB, derived by overlapping green areas in the top and bottom plots.

for the origin of deep earthquakes, the hypothesis of transformational faulting in metastable peridotite wedges requires a cold slab with thermal parameter greater than 5000 km [20]. The slab in central Taiwan is probably not cold enough for generating deep earthquakes, because the ceased subduction has warmed up the slab. Therefore, we attribute the absence of deep and intermediate-depth earthquakes beneath central Taiwan to cessation of subduction due to arc–continent collision.

6. Conclusions

First arrival P waves from Tonga–Kermadec deep and intermediate-depth earthquakes exhibit reduced amplitudes and travel times for central Taiwan stations relative to KMNB in the 0.1–0.4 Hz band. The combination of amplitude and travel time anomalies, azimuthal dependence of amplitude patterns, and correlation of amplitudes with earthquake latitudes favor receiver-side mantle anomalies over crustal effects to explain observations at central Taiwan stations. This positive correlation is consistent with the effects of an eastern dipping aseismic slab. We interpret the lack of intermediate-depth and deep earthquakes as a result of ceased subduction due to collision, resulting starvation of hydrous minerals in the dehydration embrittlement process and a warm subducting slab. Upon numerical modeling, a planar slab with 400-km-long, 4% velocity anomalies or 500-km-long, 3.2% velocity anomalies, would generate both the amplitude and travel time residuals observed at SSLB and TPUB.

Acknowledgements

We thank E. A. Okal, R. D. van der Hilst, and two anonymous reviewers for improving the manuscript.

References

[1] B.H.T. Chai, Structure and tectonic evolution of Taiwan, Am. J. Sci. 272 (1972) 389–422.
[2] C.S. Ho, A synthesis of the geologic evolution of Taiwan, Tectonophysics 125 (1986) 1–16.
[3] L.S. Teng, Geotectonic evolution of Late Cenozoic arc–continent collision in Taiwan, Tectonophysics 183 (1990) 57–76.

[4] S. Lallemand, Y. Font, H. Bijwaard, H. Kao, New insight on 3-D plate interaction near Taiwan from tomography and tectonic implications, Tectonophysics 335 (2001) 229–253.
[5] S.K. Hsu, J.C. Sibuet, Is Taiwan the result of arc–continent or arc–arc collision? Earth Planet. Sci. Lett. 136 (1995) 315–324.
[6] J. Suppe, Mechanics of mountain building and metamorphism in Taiwan, Geol. Soc. China 4 (1981) 67–89.
[7] C.H. Lin, Active continental subduction and crustal exhumation: the Taiwan orogeny, Terra Nova 14 (2002) 281–287.
[8] F.T. Wu, R.J. Rao, D. Salzberg, Taiwan orogeny: thin-skinned or lithospheric collision? Tectonophysics 274 (1997) 191–220.
[9] J.E. Vidale, Waveform effects of a high-velocity, subducted slab, Geophys. Res. Lett. 14 (1987) 542–545.
[10] R.D. van der Hilst, S. Widiyantoro, E.R. Engdahl, Evidence for deep mantle circulation from global tomography, Nature 386 (1997) 578–584.
[11] K.L. Pankow, T. Lay, Modeling S wave amplitude patterns for events in the Kurile slab using three-dimensional Gaussian beams, J. Geophys. Res. 107 (B8) (2002) DOI:10.1029/2001JB000594.
[12] V.F. Cormier, Slab diffraction of S waves, J. Geophys. Res. 94 (1989) 3006–3024.
[13] B.S. Huang, A program for two-dimensional seismic wave propagation by the pseudospectrum method, Comput. Geosci. 18 (1992) 289–307.
[14] H. Kao, P.R. Jian, K.F. Ma, B.S. Huang, C.C. Liu, Moment tensor inversion for offshore earthquakes east of Taiwan and their implications to regional collision, Geophys. Res. Lett. 25 (1998) 3619–3622.
[15] P.-F. Chen, C.R. Bina, E.A. Okal, A global survey of stress orientations in subducting slabs as revealed by intermediate-depth earthquakes, Geophys. J. Int. 159 (2004) 721–733.
[16] B.L.N. Kennett, E.R. Engdahl, Travel times for global earthquakes location and phase identification, Geophys. J. Int. 105 (1991) 429–465.
[17] H.W. Green, H. Houston, The mechanics of deep earthquakes, Annu. Rev. Earth Planet. Sci. 23 (1995) 169–213.
[18] S.H. Kirby, E.R. Engdahl, R. Denlinger, Intermediate-depth intraslab earthquakes and arc volcanism as physical expressions of crustal and uppermost mantle metamorphism in subducting slabs, in: G.E. Bebout, D.W. Scholl, S.H. Kirby, J.P. Platt (Eds.), Subduction: Top to Bottom, American Geophysical Union, Washington, DC, 1996, pp. 195–214.
[19] P.F. Chen, C.R. Bina, E.A. Okal, Variations in slab dip along the subducting Nazca plate, as related to the stress patterns and moment release of intermediate-depth seismicity and to surface volcanism, Geochem. Geophys. Geosyst. 2 (2001) DOI:10.1029/2001GC000153.
[20] S.H. Kirby, S. Stein, E.A. Okal, D.C. Rubie, Metastable phase transformations and deep earthquakes in subducting oceanic lithosphere, Rev. Geophys. 34 (1996) 261–306.